# Exploration of copper-free ZnTe buffer layers for CdTe-based solar cells

Yegor Samoilenko and Colin A. Wolden Colorado School of Mines, Golden, CO 80401, USA

Abstract — Development of copper-free ZnTe buffer layers for CdTe-based solar cells is an important avenue for improving stability. Group V elements offer a path towards that goal. This work explores two group V elements, phosphorous and antimony, as candidates for making copper-free p-type ZnTe buffer layer using thermal evaporation. It is found that incorporation of both elements into ZnTe film can easily be done. In addition, asdeposited ZnTe films are Te-rich and Cd<sub>1-x</sub>Zn<sub>x</sub>Te alloys form upon co-evaporation of ZnTe and Cd<sub>3</sub>P<sub>2</sub>, improving crystallinity and stoichiometry of the film. Activation of P poses a challenge, while ZnTe films with Sb produced good sheet resistance values.

Index Terms — buffer layer, cadmium telluride, doping, tellurium, zinc telluride.

## I. INTRODUCTION

Cadmium telluride (CdTe) has become the leading thin-film photovoltaic (PV) technology with record device efficiency currently at 22.1% [1]. One of the challenges in CdTe is creating a good ohmic contact due to its high work function and low carrier concentration. It is well known that ZnTe can be easily doped p-type using group V elements [2]. Its valence band alignment with CdTe and wider band gap makes it an ideal back contact buffer layer for CdTe solar cells to create an ohmic contact between CdTe and metal layers [3]. First Solar has attributed improvements in both efficiency and reliability to the integration of ZnTe buffer layer in their device stack [4]. The common dopant that is used in the buffer layer is copper [5]. However, incorporation of Cu poses stability concerns as Cu can diffuse into the bulk and to the front contact interface, creating recombination centers. Therefore, developing Cu-free back contacts is one of the grand challenges for CdTe solar cells. Introduction of group V dopants into the ZnTe buffer layer can be a potential way to overcome this challenge [6],[7]. Although examples of doping ZnTe are present in the literature, most of them are done in a way that is not commercially viable, such as MBE. In this work we are exploring ways of doping ZnTe with phosphorous and antimony in a cost-effective way.

## II. MATERIALS AND METHODS

ZnTe thin films were deposited by thermal evaporation onto a glass substrate. To introduce phosphorous or antimony into the film,  $Cd_3P_2$  or Sb were used as sources, respectively. For

most experiments, substrate temperature was held at 100 °C. The thickness of the films was monitored using quartz monitor crystals (QCMs) and was measured by profilometry and was ~450-500 nm for most films. Rapid thermal processing (RTP) oven with nitrogen ambient was used for annealing. X-ray diffraction (XRD) with Cu source was used to analyze the structure of the as-deposited and annealed films. UV-Vis spectophotometry in the 400-1500 nm range was employed to study optical properties. 4-point probe and Hall measurements were done to determine the electrical properties of the films.

### III. RESULTS AND DISCUSSION

## A. As-deposited ZnTe

To co-evaporate ZnTe along with a source of group V dopant the rate of ZnTe deposition needs to be significantly higher to keep the dopant loading at reasonable values. However, ZnTe film quality would degrade as deposition rate is increased. In our standard devices with ZnTe:Cu buffer layers the rate of ZnTe deposition is ~5 A/s at 100°C substrate temperature [5]. Pure ZnTe films were deposited at different rates to evaluate the quality of the films for future experiments. Fig. 1 illustrates XRD patterns and transmission spectra as a function of deposition rate, as well as Tauc plots for band gap determination.

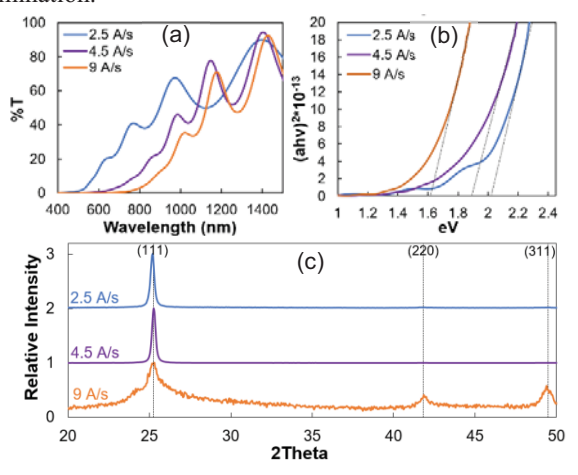


Fig. 1. ZnTe films deposited at 100°C as a function of deposition rate: a) Transmission spectra; b) Tauc plot; c) XRD patterns.

As can be seen from the XRD patterns, crystallinity is improved dramatically when rate is reduced from 9 A/s down to 4.5 A/s as evidenced by narrowing of (111) peak. However, transmission spectra illustrate that band gap of all the films are below theoretical value of 2.26 eV. This could be due to presence of excess Te, which is consistent with literature that suggests excess Te presence for ZnTe films deposited at substrate temperatures below 300°C [8]-[10] as well as our recent work on interdiffusion of CdTe and ZnTe thin films [11]. ZnTe deposition rate of 2.5 A/s produced best films with band gap being closest to theoretical value of 2.26 eV. Therefore, rate of 2.5 A/s was used for all further experiments in this paper.

## B. Phosphorous incorporation

Fig. 2 below shows UV-Vis and XRD for both pure ZnTe and one of ZnTe:  $Cd_3P_2$  films. Thickness of co-evaporated  $Cd_3P_2$  was ~3.5 vol% of ZnTe film. There are a couple interesting things can be noticed from the figure. First, (111) peak shifts to lower value for ZnTe:  $Cd_3P_2$  sample, which suggests formation of  $Cd_{1-x}Zn_xTe$  (CZT) alloy. Secondly, although CZT is forming, the band gap of the film moves in the opposite direction relative to the pure ZnTe film. This can be explained by the presence of excess Te in ZnTe film. This excess Te lowers the effective band gap of ZnTe film. Presence of Cd in evaporation chamber prevents excess Te and forms CZT alloy with ZnTe. Band gap of ~2.1 eV is relatively consistent with (111) peak position ~25.1 which translates into alloy composition of  $Cd_{0.13}Zn_{0.87}Te$ .

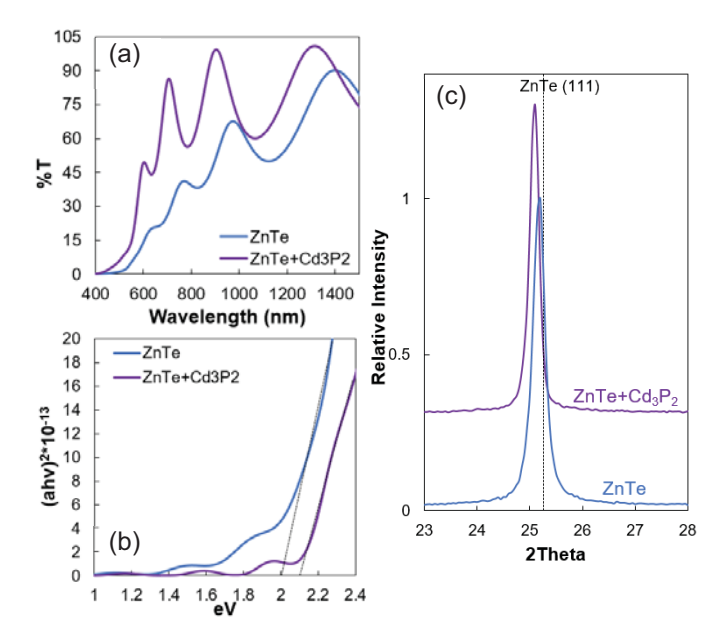


Fig. 2. ZnTe co-evaporated with  $Cd_3P_2$  at  $100^{\circ}C$ : a) Transmission spectra; b) Tauc plot; c) (111) XRD peak position.

Even though presence of phosphorous cannot be seen in XRD patterns, it was confirmed by EDAX measurements as well as ICP-MS. Cd/P ratio based on EDAX measurements came out in the 1.8-2.3 range. Therefore, incorporation of phosphorous

can be done by co-evaporation of ZnTe and Cd<sub>3</sub>P<sub>2</sub>. However, activating it poses a challenge. ZnTe:Cd<sub>3</sub>P<sub>2</sub> films were annealed in the RTP chamber using 60 second anneals at 25°C increments in the temperature range between 350 and 475 °C. 4-point probe measurements were performed after each annealing step. However, the films were too resistive to produce a reading even at the highest annealing temperature. Increasing temperature past 425°C also resulted in gradual discoloration of the films. Lower loadings of P, higher substrate temperatures and longer anneal times will be explored in efforts to produce p-type ZnTe:P films.

## C. Antimony incorporation

Barati et. al. [12] produced ZnTe films with low sheet resistance by sandwiching a thin layer of Sb between ZnTe layers and annealing for 1 hr at 320°C. To achieve good crystallinity and low resistivity the authors had to use elevated substrate temperature of 420°C for first ZnTe layer. In our experiments we utilized similar method for making ZnTe:Sb films but at a low substrate temperatures of 100 °C for ZnTe deposition and ~12 °C for Sb deposition. Fig. 3 below illustrates sheet resistance as a function of Sb volume fraction. Interestingly, both as-deposited and annealed films have similar sheet resistance values at Sb loadings above 2.5%.

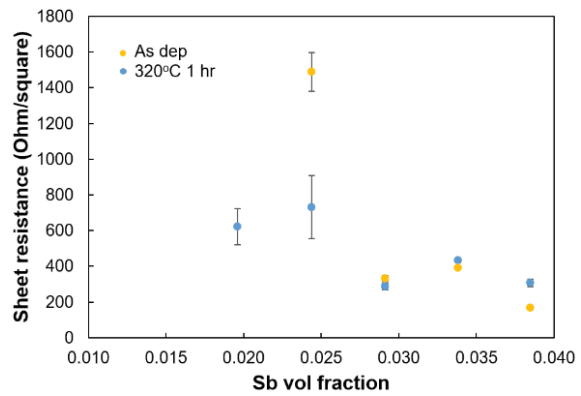


Fig. 3. Sheet resistance of as-deposited and annealed ZnTe|Sb|ZnTe films as a function of Sb volume fraction.

Hall measurements were performed to determine carrier concentration and mobility in ZnTe/Sb/ZnTe films. Fig. 4 below shows carrier concentration and mobility for asdeposited and annealed at 320°C for 1 hr films as a function of Sb content. All films show p-type behavior. As-deposited films exhibit high carrier concentrations on the order of 10<sup>19</sup> cm<sup>-3</sup>, increasing only slightly with increasing Sb content. Surprisingly the mobility in as-deposited films improves with increasing Sb content from below 10 to above 50 cm<sup>2</sup>/V-s. Interestingly, carrier concentration drops almost in half to 10<sup>18</sup> cm<sup>-3</sup> range upon annealing, while mobility improves for most samples.

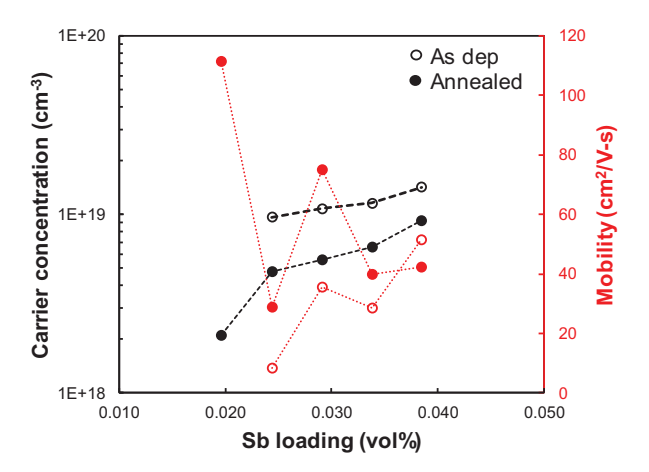


Fig. 4. Carrier concentration and mobility as a function of Sb content for as-deposited and annealed at 320°C for 1 hr for ZnTe/Sb/ZnTe samples.

To better understand the structural changes that occur during an annealing step Fig. 5 shows XRD patterns of as-deposited and annealed ZnTe/Sb/ZnTe films. As can be seen from the figure, as-deposited film has a peak at 23.65° which corresponds to Sb. This peak disappears for annealed sample and two peaks at ~26.3 and 44.7° that correspond to Sb<sub>2</sub>Te<sub>3</sub> appear. The presence of Sb<sub>2</sub>Te<sub>3</sub> seems to suggest that excess Te in ZnTe films reacts with Sb upon annealing. Most likely a thin Sb film that is in between ZnTe layers in as-deposited sample provides an electrical path and is responsible for low resistivity and high carrier concentration. Mobility improvement with increasing Sb content in as-deposited films is consistent with this idea. Homogeneity of Sb sandwiched in-between ZnTe films would be improved as it gets thicker.

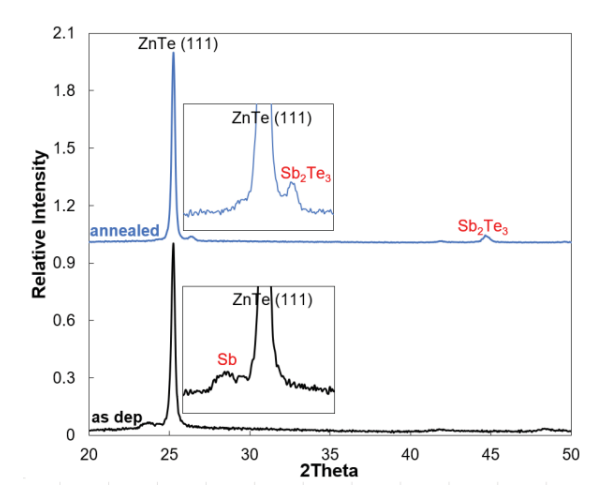


Fig. 5. XRD patterns of as-deposited and annealed at 320 °C for 1 hr ZnTe|Sb|ZnTe films with 3 vol% Sb. Magnification near ZnTe (111) is provided to show Sb and Sb<sub>2</sub>Te<sub>3</sub> peaks.

Co-evaporation of ZnTe with Sb and annealing those films did not produce any 4-point probe measurements at this moment. Fig. 6 shows XRD patterns of as-deposited and annealed films for co-evaporated ZnTe:Sb films. Although

Sb<sub>2</sub>Te<sub>3</sub> forms upon annealing, it doesn't seem to provide same electrical benefits in co-evaporated films as it does in "sandwiched" films. One of the possible explanations could be that in co-evaporated films Sb<sub>2</sub>Te<sub>3</sub> is spread out across the entirety of ZnTe film, while in other case it stays in-between ZnTe layers and provides electrical path in a fashion similar to Sb in as-deposited films. This would be consistent with the fact that Sb<sub>2</sub>Te<sub>3</sub> films were shown to exhibit p-type behavior with carrier concentrations well into 10<sup>19</sup> cm<sup>-3</sup> [13]. Cross sectional TEM analysis could shine light on whether Sb<sub>2</sub>Te<sub>3</sub> that forms upon annealing remains in-between ZnTe layers or forms clusters throughout the whole film.

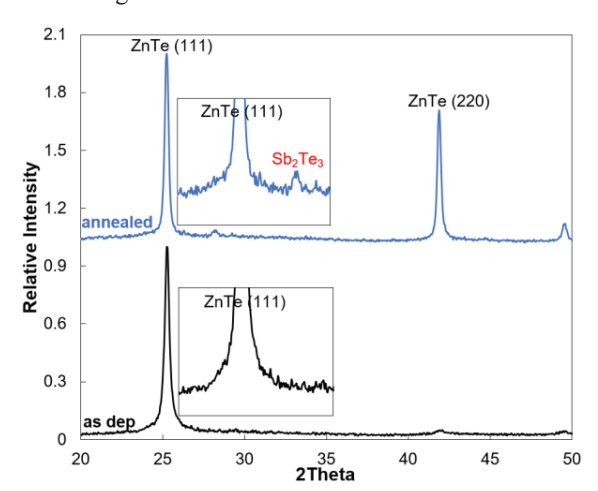


Fig. 6. XRD patterns of as-deposited and annealed at 320 °C for 1 hr co-evaporated ZnTe:Sb films with 3.5 vol% Sb. Magnification near ZnTe (111) is provided to show Sb<sub>2</sub>Te<sub>3</sub> peak.

Fig. 7 illustrates SEM image of the top surface of annealed ZnTe/Sb/ZnTe sample with 3% Sb. Although total thickness of the film is  $\sim$ 500 nm, the surface is smooth and grains are very small even after annealing, with average grain size of  $\sim$ 10 nm.

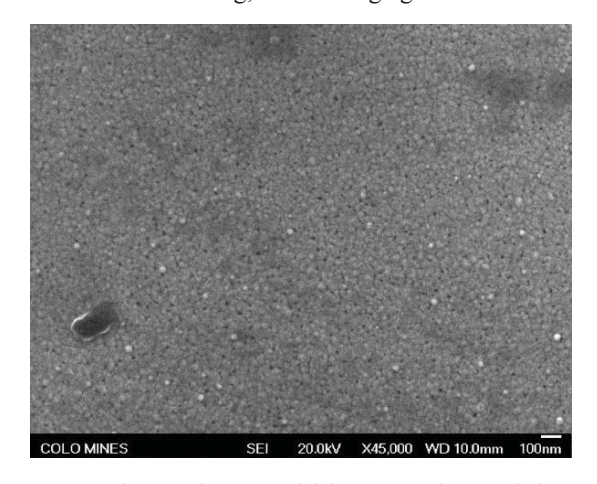


Fig. 7. SEM image of 3% ZnTe/Sb/ZnTe sample annealed at 320°C for 1 hr.

### IV. SUMMARY AND CONCLUSIONS

In this paper we demonstrate initial results of the exploration of copper-free ZnTe buffer layers for CdTe-based solar cells. Two group V elements, namely phosphorous and antimony, were successfully incorporated into ZnTe films using thermal evaporation. Films with phosphorous exhibit high resistivity with no 4-point probe readings, while certain Sb containing films show promising electrical properties. Upon annealing of ZnTe/Sb/ZnTe and ZnTe:Sb films formation of Sb<sub>2</sub>Te<sub>3</sub> is observed. However, Hall measurements seem to suggest that Sb<sub>2</sub>Te<sub>3</sub> in "sandwiched" structure is p-type and provides an electrical path while in co-evaporated ZnTe:Sb films it is most likely spread out across the entirety of ZnTe films and doesn't result in any electrical benefits.

### **ACKNOWLEDGMENTS**

We are grateful to the National Science Foundation through award number CBET-1706149. In addition, we would like to thank Joel Duenow and Matthew Reese at the National Renewable Energy Laboratory for providing access to Hall measurements.

### REFERENCES

- [1] "Best Research-Cell Efficiencies," NREL, 2016. Online at: http://www.nrel.gov/pv/assets/images/efficiency\_chart.jpg.
- [2] D. J. Chadi, "Predictor of P-type Doping in II-VI Semiconductor," *Physical Review B*, vol. 59, pp. 181-183, 1999
   [3] D. Rioux, D. W. Niles, and H. Höchst, "ZnTe: A potential
- [3] D. Rioux, D. W. Niles, and H. Höchst, "ZnTe: A potential interlayer to form low resistance back contacts in CdS/CdTe solar cells," *Journal of Applied Physics*, vol. 73, p. 8381, 1993.

- [4] L. T. Nicholas Strevel, Chad Kotarba, Imran Khan, "Improvements in CdTe Module Reliability and Long-Term Degradation Through Advances in Construction and Device Innovation," *Photovoltaics International*, vol. 22, pp. 1-8.
- [5] J. Li, D. R. Diercks, T. R. Ohno, C. W. Warren, M. C. Lonergan, J. D. Beach, et al., "Controlled activation of ZnTe:Cu contacted CdTe solar cells using rapid thermal processing," Solar Energy Materials and Solar Cells, vol. 133, pp. 208-215, 2015.
- [6] H. I. Yuji Hishida, Tadao Toda and Tatsuhiko Nilna, "Growth and Characterization of MBE-Grown ZnTe:P," *Journal of Crystal Growth*, vol. 95, pp. 517-521, 1989.
- [7] T. Baron, K. Saminadayar, and N. Magnea, "Nitrogen doping of Te-based II–VI compounds during growth by molecular beam epitaxy," *Journal of Applied Physics*, vol. 83, pp. 1354-1370, 1998
- [8] B. Späth, J. Fritsche, A. Klein, and W. Jaegermann, "Nitrogen doping of ZnTe and its influence on CdTe/ZnTe interfaces," *Applied Physics Letters*, vol. 90, p. 062112, 2007.
- [9] R. D. Feldman, R. F. Austin, P. M. Bridenbaugh, A. M. Johnson, W. M. Simpson, B. A. Wilson, et al., "Effects of Zn to Te ratio on the molecular-beam epitaxial growth of ZnTe on GaAs," *Journal of Applied Physics*, vol. 64, pp. 1191-1195, 1988.
  [10] G. K. Rao, K. V. Bangera, and G. K. Shivakumar, "The effect of
- [10] G. K. Rao, K. V. Bangera, and G. K. Shivakumar, "The effect of substrate temperature on the structural, optical and electrical properties of vacuum deposited ZnTe thin films," *Vacuum*, vol. 83, pp. 1485-1488, 2009.
- [11] Y. Samoilenko, A. Abbas, J. Michael Walls, and C. A. Wolden, "Copper-induced recrystallization and interdiffusion of CdTe/ZnTe thin films," *Journal of Vacuum Science & Technology A: Vacuum, Surfaces, and Films*, vol. 36, p. 031201, 2018.
- [12] A. Barati, A. Klein, and W. Jaegermann, "Deposition and characterization of highly p-type antimony doped ZnTe thin films," *Thin Solid Films*, vol. 517, pp. 2149-2152, 2009.
- [13] H. Zou, D. M. Rowe, and G. Min, "Preparation and characterization of p-type Sb<sub>2</sub>Te<sub>3</sub> and n-type Bi<sub>2</sub>Te<sub>3</sub> thin films grown by coevaporation," *Journal of Vacuum Science & Technology A: Vacuum, Surfaces, and Films*, vol. 19, pp. 899-903, 2001.